Available online at www.sciencedirect.com
ScienceDirect
Journal of Power Sources 161 (2006) 138–142
JOURNAL OF POWER SOURCES
www.elsevier.com/locate/jpowsour

Short communication

Electrochemical impedance investigation of flooding in micro-flow channels for proton exchange membrane fuel cells

Suk Won Cha [a,*], Ryan O'Hayre [b], Yong-Il Park [c], F.B. Prinz [b]

[a] School of Mechanical & Aerospace Engineering, Seoul National University, San 56-1, Shinlimdong, Kwanakgu, Seoul 151-744, Republic of Korea
[b] Department of Mechanical Engineering, Stanford University, Rapid Prototyping Laboratory, Building 530, Room 226, Stanford, CA 94305-3030, United States
[c] School of Materials and System Engineering, Kumoh National Institute of Technology, 188 Shinpyung-dong, Gumi, Kyungbuk 730-701, Republic of Korea

Received 1 February 2006; accepted 11 April 2006
Available online 13 June 2006

Abstract

A study is made of the transport phenomena related to fluid flow through proton exchange membrane fuel cells (PEMFCs) that have micro-channels. Specifically, transport is investigated in channels of 100 μm and smaller, which are constructed using a structural photopolymer (SU-8). It has been suggested by other workers that fuel cell micro-channels may suffer from flooding if flow channels are too small (<100 μm). In order to confirm or reject this hypothesis, the electrochemical impedance technique has been employed to measure the mass transfer resistance. In smaller channels, mass transportation resistance is found to increase due to flooding, but that this effect may be offset by a reduction in dead zone area.

Keywords: Proton exchange membrane fuel cell; Micro-channels; Electrochemical impedance; Flooding; Mass transport resistance

1. Introduction

Recently, miniature fuel cells have emerged as promising alternative power sources for portable electronics. Various microfabrication techniques have been adopted in an effort to miniaturize fuel cells. Successful prototypes have been produced by integrating micro-flow structures based on silicon, printed-circuit boards, photopolymers, etc. [1–6]. Especially, low-cost fabrication and rapid prototyping with structural photopolymer has facilitated the investigation of micro-scale transport phenomena in flow channels, leading to the observation of significant scaling effects [1,2].

Specifically, observations of flow channel scaling have revealed that fuel cell performance is maximized at a certain channel size. Below this optimum limit there is a decrease in fuel cell performance despite the improved mass transport brought about by a reduced dead zone and increased convection [2]. It has been suggested that flooding in flow channels is responsible for the phenomena, as water-blocking effects are more severe in smaller channels and eventually inhibit oxygen access.

Electrochemical impedance has been widely used to investigate various transport phenomena in fuel cells [7,8]. Faradaic resistance will increase with increased channel flooding due to blockage of the active area of the membrane–electrode assembly by liquid water. Therefore, Faradaic resistance is used in this study as an indicator of fuel cell flooding. Additionally, because the gas-diffusion layer (GDL) thickness will also impact fuel cell flooding, changes in the Faradaic resistance due to changing GDL thickness are also monitored.

2. Experimental

Micro-flow channels were fabricated with a SU-8 photoresist (Microchem Corp.) using standard photolithography techniques. The fabrication procedures have been explained in previous papers [1,2]. Two prototype structures of flow channel were prepared with 20 and 100 μm characteristic dimensions. Both prototypes employed a parallel-flow pattern. Additionally, a macro flow structure was fabricated from a metal block by a conventional machining process. The dimensions of the flow channels are summarized in Table 1.

* Corresponding author. Tel.: +82 2 880 1700; fax: +82 2 883 1513.
E-mail addresses: swcha@snu.ac.kr (S.W. Cha), rohayre@stanford.edu (R. O'Hayre), yipark@kumoh.ac.kr (Y.-I. Park), fbp@cdr.stanford.edu (F.B. Prinz).

0378-7753/$ – see front matter © 2006 Elsevier B.V. All rights reserved.
doi:10.1016/j.jpowsour.2006.04.123

Table 1
Geometric dimensions of parallel flow channels in fuel cells

Sample no.	Channel width (μm)	Channel height (μm)	Rib width (μm)	Rib height (μm)
1	20	20	20	20
2	100	100	100	100
3	500	500	500	500

As the channels and ribs have a square profile, they have the same width. The length and width of the flow field were 12 and 14 mm, respectively. The flow inlet and outlets, which consisted of 14 mm × 1 mm pockets, were machined directly on the flow plates. Accordingly, the gas enters perpendicular to the flow channels. The dimension of active area was 14 mm × 14 mm, including flow inlet, outlet and flow channels, to give an active area of 2 cm^2. It should be noted that in all samples, the flow channel and rib *shape* were unchanged; they were only scaled in direct proportion.

The method used to test the performance of the micro-flow channels was similar to that used for conventional fuel cell stacks. Membrane–electrode assemblies (MEAs) were obtained from a commercial supplier (BCS Technology, Byran, TX) and were employed in all experiments without modification. The MEAs were composed of Nafion® 115 membrane, carbon cloth electrodes, and 1 mg cm^{-2} of Pt/C catalyst. The MEA active area was 14 mm × 14 mm (2 cm^2), i.e., the same as the flow fields.

In addition to conventional carbon-cloth based MEAs, two types of carbon paper (TGPH-120 and TGPH-30) from E-TEK, Inc., were used as GDLs. The carbon papers had nominal thicknesses of 350 μm (TGPH-120) and 90 μm (TGPH-30), respectively. Both carbon papers contained 20 wt.% PTFE for hydrophobic characteristics. For tests with the carbon paper, the carbon cloth electrodes used in the original MEAs were peeled off. Then, the carbon papers were added. The MEA was slightly pressed to regain integrity. The rest of the fuel-cell assembly and test procedures remained the same.

The MEA was sandwiched between two micro-flow plates, thin silicon rubber gaskets, and two metal blocks. The metal blocks provided gas routing for fuel and oxidant. The assembled structure was compressed with an arbor press to standardize the clamping force. A single MEA was used for measurements to minimize the variation between tests.

Pure hydrogen and air were used in all tests. The flow rates of hydrogen and air were 50 and 100 sccm under atmospheric pressure, respectively. Both gases were fully saturated at 50 °C before entering the fuel cell.

Current–voltage (*I–V*) measurements were repeated several times until steady-state performance were obtained. The resulting *I–V* curves were obtained using a Solartron 1287 potentiostat and a 1260 Impedance/Gain-Phase Analyzer. The ac impedance was measured with the same equipment at constant voltage. A sinusoidal signal with an amplitude of 10 mV was applied to the fuel cells. The impedance response was measured at 0.8, 0.6 and 0.3 V to explore the low, medium and high current density operating regimes. The frequency of the sinusoidal signal was swept between 100 kHz and 0.1 Hz.

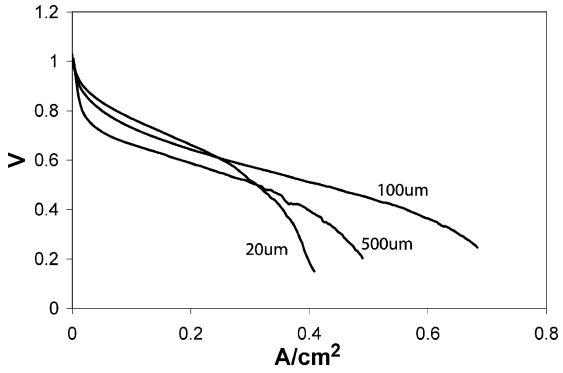

Fig. 1. IR-free cell polarization curves for different flow channel samples. A commercial MEA (Nafion 115 with 1 mg cm^{-2} Pt/C catalyst on carbon cloth) was used. IR losses, measured from ac impedance, have been subtracted from the curves.

3. Results and discussion

3.1. Effect of flow channel size on Faradaic impedance

Cell polarization curves for the 500, 100 and 20 μm flow channels using the same commercial MEA are shown in Fig. 1. In these curves, the IR losses have been corrected by subtracting the high-frequency resistance measured from the ac impedance. Thus, the curves show mainly activation and mass transport losses. Fuel cell performance increases as the channel size decreases from 500 to 100 μm. By contrast, performance decreases for the 20-μm channel. The initial increase of performance with channel size has previously been suggested [2] to result from improved convective mass transport in smaller channels due to increased gas velocity (since total mass flow rate is fixed but the total area of the flow channels decreases as the channel size decreases). Also, the dead zone area (under the rib) decreases with decreasing channel size [2]. The decrease in performance for a channel size of 20 μm is considered to be due to water-blocking (or flooding) effects in the channels [2].

Nyquist plots of the three fuel cells are shown in Fig. 2. The Faradaic resistance for the 500-μm channels is greatest at 0.8 V but decreases as the operating voltage decreases to 0.6 V. This trend is commonly observed in fuel cells due to increased charge transfer at the catalyst. At 0.3 V, the resistance increases slightly compared with that at 0.6 V. The decrease in charge-transfer resistance as the overvoltage increases shows that mass-transport resistance has increased due to lack of oxygen in the flooded flow channel and GDL [7,8]. Interestingly, the 100-μm channels exhibit a consistent decrease in Faradaic resistance as the operation voltage decreases. This implies that this channel has better mass transport, or less flooding, at higher current densities due to a reduced dead zone and increased gas velocity.

In 20-μm channels, the impedance loop diameter increases when the applied voltage is changed from 0.6 to 0.3 V. It is considered that this increase in Faradaic impedance is caused by increasing mass-transport overvoltage due to flooding. Small channels may be more susceptible to flooding because the trapped water blocks a relatively larger area due to the small free volume of the channels [1,2]. These impedance results confirm

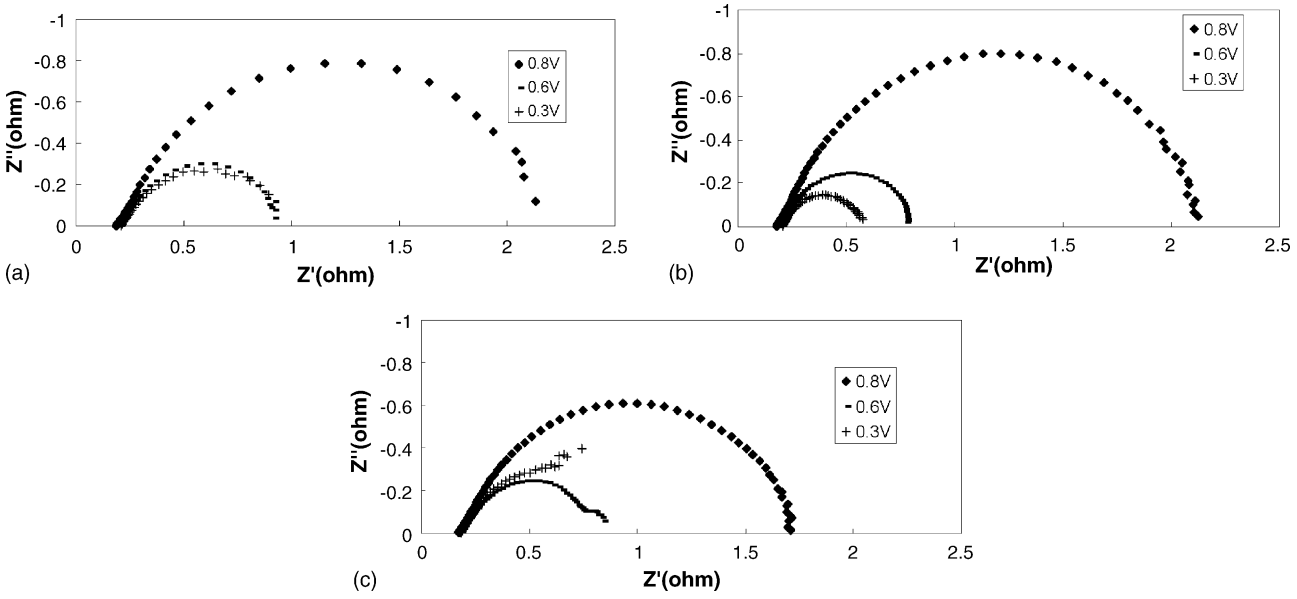

Fig. 2. Measurements of ac impedance from different flow channel sizes at different operation voltages: (a) 500-μm, (b) 100-μm and (c) 20-μm channels. A commercial MEA (Nafion 115, carbon cloth with 1 mg cm^{-2} Pt/C) was used.

the trends observed in the polarization curves shown in Fig. 1. Similar trends have been observed using the current interruption method [2].

The experimental data from Fig. 2 are rearranged in Fig. 3 at the same loading voltage to compare the difference of Faradaic impedance among different channels. Also, the ohmic resistance has been removed from the data to facilitate easy comparison of the Faradaic loops.

Interestingly, at high voltage (0.8 V, Fig. 3(a)), the 20-μm channel shows significantly lower Faradaic impedance. It has been suggested [2] that the high-pressure drop in very small flow channels improves air convection into the GDL, and thus improves fuel cell performance at low current density (high voltage). The polarization curve of the 20-μm channel from Fig. 1 confirms this suggestion as the output voltage is relatively high voltage at low current density.

3.2. *Effect of GDL thickness on Faradaic impedance*

Mass transport in fuel cells depends not only on the flow channel geometry, but also on the coupling between the flow channel and the GDL. Therefore, to explore further micro-scale mass transfer effects, alternative GDLs were examined.

So, why is performance degradation in the smallest channels no longer observed, compared with the carbon cloth GDL experiments? Since the carbon cloth is softer than the carbon papers,

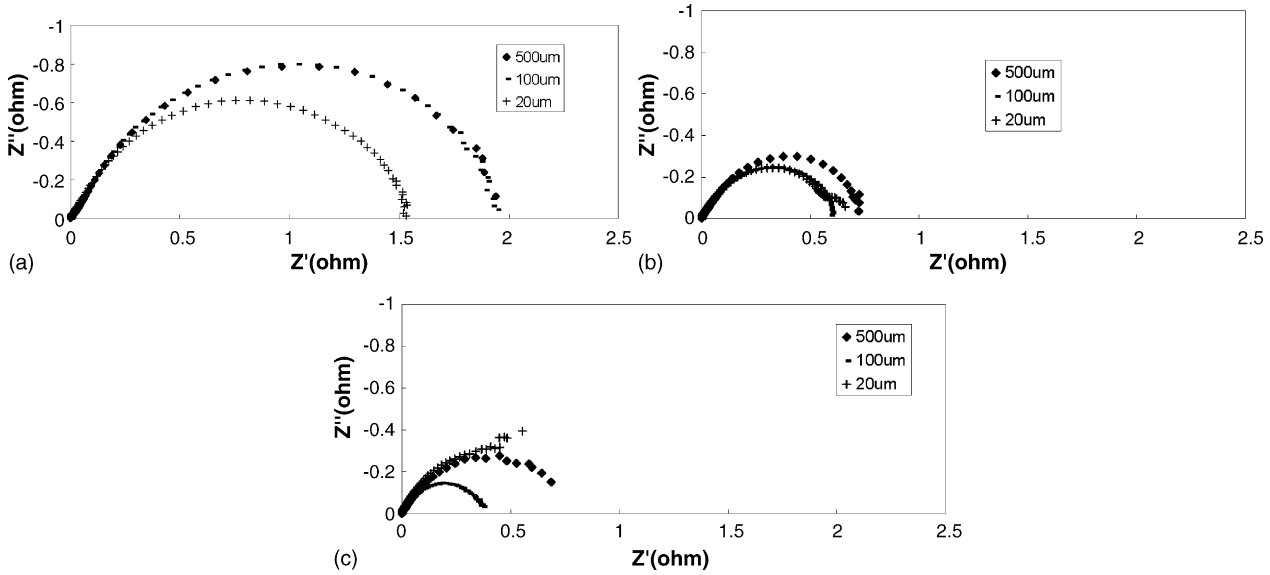

Fig. 3. Measurements of ac impedance for different micro-flow channels at various operation voltages: (a) 0.8 V, (b) 0.6 V and (c) 0.3 V. To obtain these curves, the data from Fig. 2 have been rearranged in terms of operating voltage. High-frequency resistances have been removed from original data to facilitate comparison of Faradaic impedances.

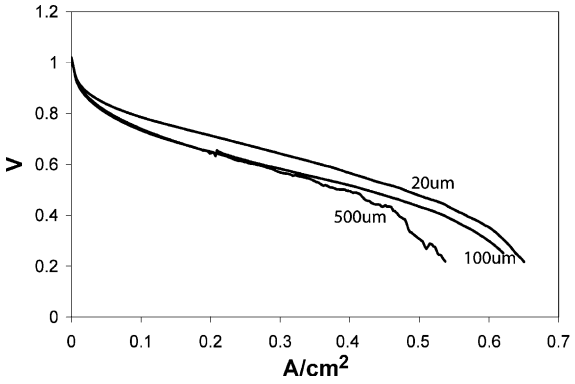

Fig. 4. IR-corrected cell polarization curves for different fuel cell samples using carbon paper (350-μm thick, 20 wt.% PTFE treated) GDLs instead of carbon cloth (350-μm thick) GDLs.

the carbon cloth may block the small channels. This effect causes a decrease in the volume of the flow channels compared with the nominal dimensions. Thus, the actual size of the channels may be much smaller. This may result in amplified flooding effects, given the flow channel size.

A set of cell polarization curves acquired from the same flow structures as in the previous experiment, but with thick (350 μm) carbon papers used as GDLs instead of the standard carbon cloth GDL, are presented in Fig. 4. Comparing these new curves with those shown previously in Fig. 1, it is noticed that there is a significant improvement in the performance of the 20-μm channels. This is attributed to the conformity difference between carbon cloth and carbon paper. Carbon cloth tends to conform easily into the flow channels, whereas carbon paper is significantly more rigid. Therefore, carbon cloth may cause significantly greater blockages in the small channels. So that the actual size of the small flow channels may be much smaller and thereby amplify flooding effects. By employing the more rigid carbon paper GDL, the blockage problem is alleviated and the degree of flooding is lowered.

When carbon cloth is employed, the 20-μm channel exhibits at 0.6 V a larger Faradaic impedance than the 100-μm channel (see Fig. 3(b)). On using carbon paper, however, the 20-μm channel shows lower impedance than the 100-μm channel (see Fig. 5). Interestingly at 0.3 V, the Faradaic impedance of the 20-μm channel is larger than that of 100-μm channels (Fig. 5). This indicates that flooding effects have not been entirely eliminated in the 20-μm channels with the switch to the carbon paper GDL.

Flooding effects can, however, be further suppressed by reducing the GDL thickness, as shown by the results given in Fig. 6 for the use of a thin (90 μm) carbon paper. As with a thick carbon paper GLD, the smallest channel (20 μm) shows the best performance. In this case, however, close inspection of the Faradaic impedance spectra shown in Fig. 7 reveals that the 20-μm channel has the lowest impedance at all voltages, as opposed to the situation with a thick carbon paper GDL.

This effect can be explained by improved diffusion in the thinner GDL. As the GDL thickness decreases, the smaller channels may benefit more since they suffer less oxygen deficiency under the ribs (note that the rib sizes are the same as the channel sizes in all prototypes). By contrast, the thin GDL causes increased dead

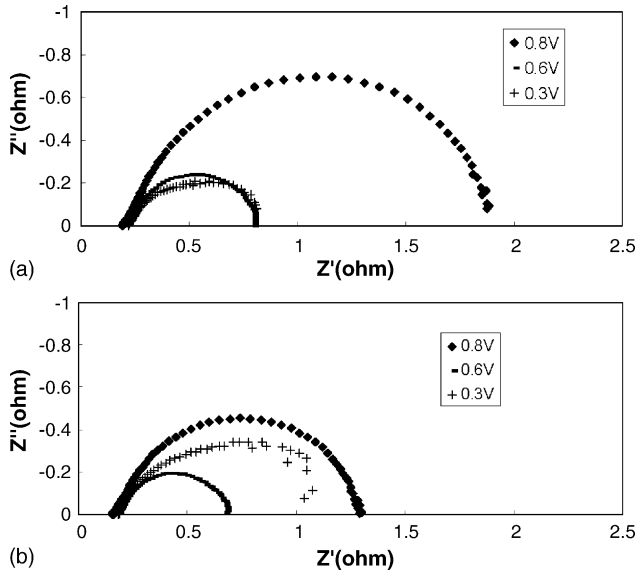

Fig. 5. Measurements of ac impedance for different flow channel sizes at various operation voltages: (a) 100-μm and (b) 20-μm channels. A 350-μm thick carbon paper used for the GDL.

zone effects, and therefore significantly decreased performance for the 500-μm channels (cf. polarization data in Figs. 4 and 6). The 100 and 20-μm channel prototypes both exhibit a decrease in the impedance loop diameter upon switching to the thinner GDL. This shows the benefit of combining micro-channel flow structures with thinner GDLs.

The observed Faradaic impedance data when using a thin carbon paper GDL (Fig. 5) or a thick carbon paper GDL (Fig. 7) are summarized in Fig. 8. In all the experiments involving the 100 and 20-μm flow channels, a decrease in Faradaic impedance is observed when the thin GLD is employed. It is concluded that this improvement results from the decreased diffusion path of the thinner GDL. Because the rib size is of the same order or smaller than the GDL thickness for the 100 and 20-μm channel prototypes, dead zone effects due to the decreased GDL thickness are negligible. On the other hand, the 500-μm channel prototype suffers significant performance degradation when employing the thinner GLD, as shown in Figs. 4 and 6, due to increased dead zone effects.

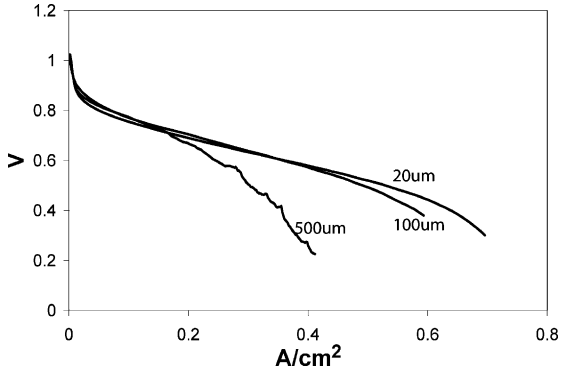

Fig. 6. IR-corrected cell polarization curves for different fuel cell samples using carbon paper (90-μm thick, 20 wt.% PTFE treated) GDLs.

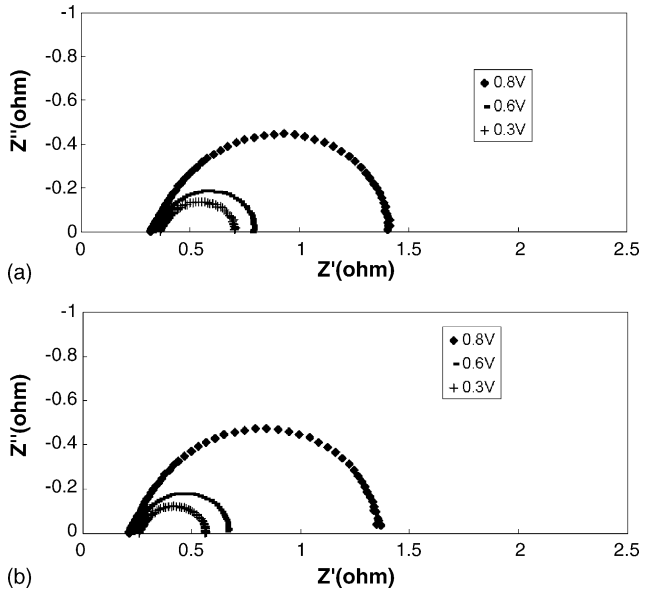

Fig. 7. Comparison of ac impedance spectra for different flow channels at various operation voltages: (a) 100-μm and (b) 20-μm channels. A 90-μm thick carbon paper used for GDL.

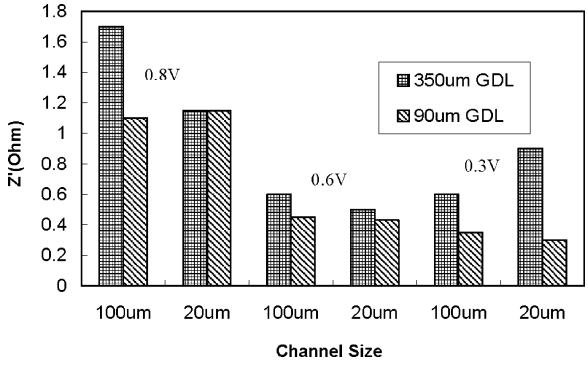

Fig. 8. Comparison of Faradaic impedances with thin (90 μm) and thick (350 μm) carbon paper GDLs at different operation voltages.

The data in Fig. 8 also imply that smaller channels benefit more from a thinner GDL, especially at high current density, since the decrease of Faradaic impedance is more dramatic in 20-μm channels. Since oxygen deficiency by flooding is most likely to occur at high current, the effect of a reduced dead zone and improved convection in smaller channels may be more prominent at high current density. Similar predictions have been made by numerical modelling using a single-phase fuel cell model in which water exists only in vapour form [2,9].

4. Conclusions

The effect of channel size and gas-diffusion layer thickness has been examined at the micro-scale. Micro-scale flow channels are more susceptible to flooding, but at the same time can provide mass transport benefits by reducing dead zones and increasing gas flow velocity. The use of a thin GDL improves the performance of micro-channels. Indeed, it appears that matching the GDL thickness to the flow channel dimensions, so that they are approximately the same, improves performance. The benefit is most prominent at high current density (low voltage). For further investigation, visualization of flooding and localized impedance technique may be combined to reveal the detailed flooding phenomena in micro-channels [10,11].

Acknowledgements

This work was supported by Honda Research Institute Inc., a Stanford Graduate Fellowship, and Korea Institute of Science and Technology.

References

[1] S.W. Cha, S.J. Lee, Y.I. Park, F.B. Prinz, Fuel cell science, engineering and technology, in: R.K. Shah, S.G. Kandliker (Eds.), Proceedings of First International Conference on Fuel Cell Science Engineering and Technology, ASME, NY, 2003, pp. 143–148.
[2] S.W. Cha, R. O'Hayre, S.J. Lee, Y. Saito, F.B. Prinz, J. Electochem. Soc. 151 (2004) A1856–A1864.
[3] R. Savinell, J. Wainright, L. Dudik, K. Yee, L. Chen, C.-C. Liu, Y. Zhang, Power source for the new millennium, in: M. Jain, M.A. Ryan, S. Surampudi, R.A. Marsh, G. Nagarajan (Eds.), Electrochemical Society Proceedings, vol. 2000-22, AZ, 2000.
[4] S.C. Kelley, G.A. Deluga, W.H. Smyrl, Electrochem. Solid-State Lett. 3 (2000) 407–409.
[5] S.J. Lee, A. Chang-Chien, S.W. Cha, R. O'Hayre, Y.I. Park, Y. Saito, F.B. Prinz, J. Power Sources 112 (2002) 410–418.
[6] R. O'Hayre, D. Braithwaite, W. Hermann, S.J. Lee, T. Fabian, S.W. Cha, Y. Saito, F.B. Prinz, J. Power Sources 124 (2003) 459–472.
[7] T.E. Springer, T.A. Zawodzinski, M.S. Wilson, S. Gottesfeld, J. Electrochem. Soc. 143 (1996) 587–599.
[8] M. Ciureanu, R. Roberge, J. Phys. Chem. B 105 (2001) 3531–3539.
[9] S.W. Cha, R. O'Hayre, Y. Saito, F.B. Prinz, J. Power Sources 134 (2004) 57–71.
[10] D.J.L. Brett, S. Atkins, N.P. Brandon, V. Vesovic, N. Vasileiadis, A. Kucernak, Electrochem. Solid State 6 (2003) A63–A66.
[11] K. Tüber, D. Pocza, C. Hebling, J. Power Sources 124 (2003) 403–414.